J|A|C|S COMMUNICATIONS

Published on Web 11/19/2009

Preferential Encapsulation and Stability of La_3N Cluster in 80 Atom Cages: Experimental Synthesis and Computational Investigation of $La_3N@C_{79}N$

Steven Stevenson,*,† Yan Ling,† Curtis E. Coumbe,† Mary A. Mackey,† Bridget S. Confait,† J. Paige Phillips,† Harry C. Dorn,‡ and Yong Zhang*,†

Department of Chemistry and Biochemistry, University of Southern Mississippi, 118 College Drive #5043, Hattiesburg, Mississippi 39406, and Department of Chemistry, Virginia Polytechnic Institute & State University, 107 Davidson Hall, Blacksburg, Virginia 24061

Received October 6, 2009; E-mail: steven.stevenson@usm.edu; yong.zhang@usm.edu

Trimetallic nitride clusters, M_3N, where M = Group IIIB and 4f-block metals, can be encapsulated in all-carbon cages (e.g., C_{80}, C_{88}, C_{96}) to form metallic nitride fullerenes (MNFs).[1−4] Of these metals, Sc has the smallest ionic radius, and $Sc_3N@C_{80}$ is readily produced as the dominant member of the MNF family of compounds (e.g., $Sc_3N@C_{68}$,[5] $Sc_3N@C_{78}$[6]). The ease of synthesizing $Sc_3N@C_{80}$ is in stark contrast to syntheses utilizing rare earth metals having larger radii. Efforts to synthesize larger metal atom trimetallic nitride clusters (i.e., $La_3N@C_{80}$) in C_{80} cages have been unsuccessful. Adjacent to La and shown in Figure 1, neighboring metal MNFs such as $Ce_3N@C_{80}$, $Pr_3N@C_{80}$, and $Nd_3N@C_{80}$ with C_{80} cages are not the preferred compounds; rather the cage size increases to the preferred C_{88} cage.[7−9] The difficulty in entrapping these bulky clusters in C_{80} cages has been attributed to larger ionic radii. For La_3N clusters, the preferred cage size shifts beyond C_{88}, and $La_3N@C_{96}$ becomes the dominant MNF.[10] In the reverse direction, from left to right (i.e., Gd, Tb, Dy, Ho, Er, Tm, and Lu), the ease and yield of making rare earth C_{80} MNFs increase as the ionic radius decreases. The smallest 4f-block based MNF, $Lu_3N@C_{80}$, is synthesized in high yield and is the dominant MNF.

In this communication, we also report the electronic stabilization of $La_3N@C_{79}N$, a molecule which represents a new class of metallic nitride azafullerenes (MNAFs).

The synthesis of $La_3N@C_{79}N$ is achieved via the CAPTEAR approach (Chemically Adjusting Plasma Temperature, Energy, and Reactivity).[11] In this method, a 0.5 in. graphite rod is core-drilled to 3/16" inch and packed with a ratio of 1.25 g of Sc_2O_3 to 3.75 g of La_2O_3. The oxidizing atmosphere and CAPTEAR conditions are achieved via addition of 2 Torr/min air into the plasma reactor. Our experiments for synthesizing $La_3N@C_{79}N$ are performed with less air (2 Torr/min) added to the reactor relative to previously published CAPTEAR conditions for synthesis of $Sc_3N@C_{80}$ (6 Torr/min).[11] Other reactor conditions include a He flow rate of 630 mL/min, 220 A, a 36 V gap, and a dynamic flow at 300 Torr. Resulting soot (11.3 g) is harvested and extracted with carbon disulfide. Upon solvent removal, the residue is washed with ether, and 20 mg of extract is obtained. A MALDI mass spectrum of this material is shown in Figure 2. The larger abundance of $LaSc_2N@C_{80}$ relative to $Sc_3N@C_{80}$ may be attributed to the slightly higher molar ratio of La to Sc within the cored graphite rod. Mass spectral results indicate an absence of $La_3N@C_{80}$, *m/z* 1391, and, surprisingly, the successful synthesis of $La_3N@C_{79}N$ (*m/z* 1393). This experimental data clearly indicate a preference of 80 atom cages of $C_{79}N$ versus C_{80} to encapsulate the La_3N cluster. The peak height of $La_3N@C_{79}N$ in the MALDI is 5% of $Sc_3N@C_{80}$. Experimental and calculated

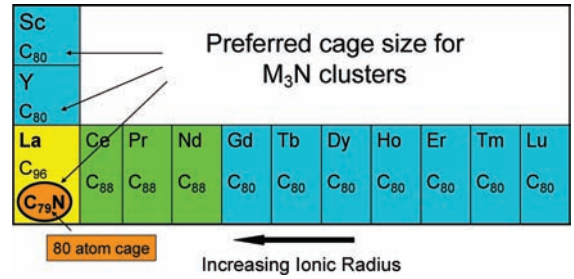

Figure 1. Overview of preferred cages for M_3N clusters with C_{80} (blue), C_{88} (green), and C_{96} (yellow). The preferred 80 atom cage for $La_3N@C_{79}N$ is circled.

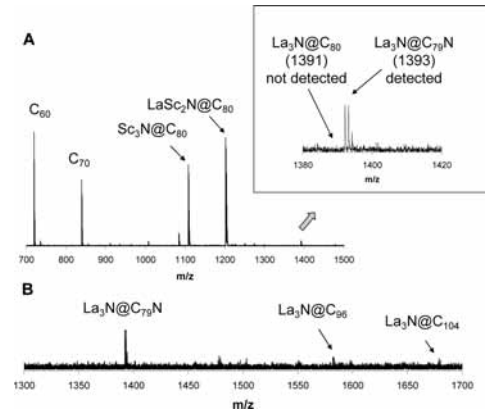

Figure 2. MALDI mass spectral data of soot extract obtained under CAPTEAR conditions.

MALDI isotope pattern distributions for $La_3N@C_{79}N$ and $La_3N@C_{96}$ are provided in the Supporting Information.

The absence of $La_3N@C_{80}$ in our soot extract is consistent with prior attempts to produce $La_3N@C_{80}$ in detectable quantities. Our experimental and computational results suggest that the La_3N cluster does not necessarily force the cage's expansion to larger sizes. The MALDI data can be interpreted to suggest that the La_3N cluster selects a smaller 80-atom cage if one of the carbon cage atoms can be substituted with nitrogen. $La_3N@C_{79}N$ dominates the product distribution, even above the yield of the otherwise preferred $La_3N@C_{96}$ (Figure 2B). For the La_3N cluster, this reduction of cage size from 96 to 80 atoms reflects the significance and role of electronic effects in lieu of ionic radius.

To understand geometric and electronic properties of the largest metallic nitride azafullerene ($M_3N@C_{79}N$, M = La) reported so far, we performed a series of density functional theory (DFT) calculations using the spin unrestricted mPW1PW91 method[12] with

† University of Southern Mississippi.
‡ Virginia Polytechnic Institute & State University.

10.1021/ja908370t

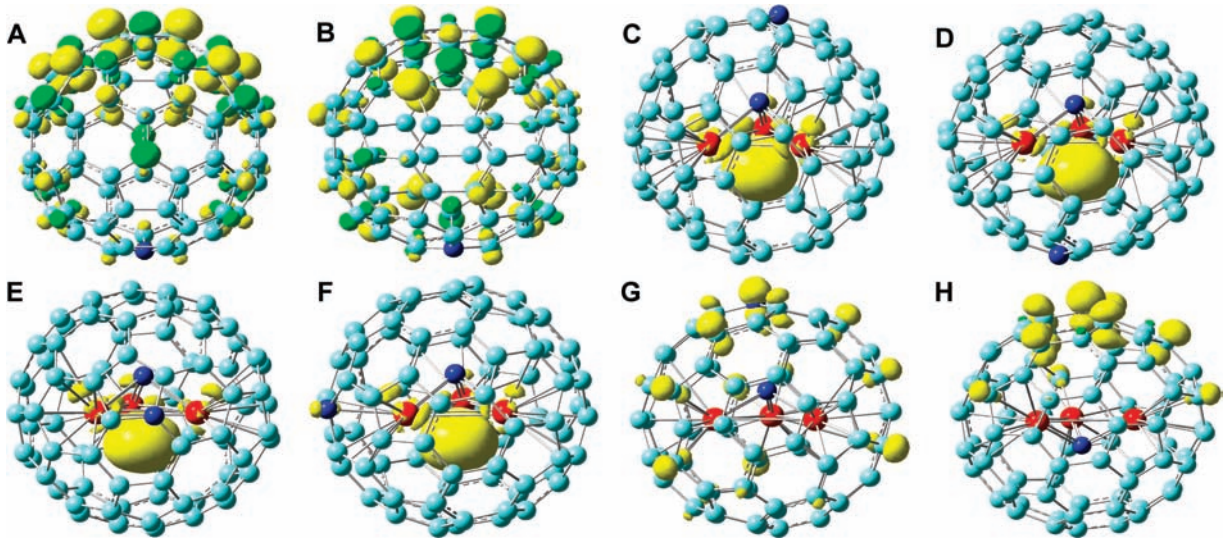

Figure 3. Isosurface representations of spin densities of $C_{79}N$ isomers **1**−**2** and $La_3N@C_{79}N$ isomers **3**−**8** in **A**−**H**, respectively (contour values = ± 0.004 au). Atom color schemes are as follows: cyan, C; blue, N; and red, La.

Table 1. Structural, Charge, Spin, and Energetic Properties of $La_3N@C_{79}N$ Isomers **3**−**8** [a]

	R_{NM} (Å)	R_{MM} (Å)	$R_{NN'}$ (Å)	$R_{N'M}^{min}$ (Å)	Σ∠MNM (deg)	Q_N (e)	Q_M (e)	$Q_{N'}$ (e)	$Q_{C'}$ (e)	ρ_N (e)	ρ_M (e)	ΔE (kcal/mol)	ΔE^{high} (kcal/mol)
3	2.188	3.124	2.971	4.212	273.3	−1.135	0.728	−0.305	0.230	−0.022	0.327	0.00	0.00
4	2.159	3.179	5.124	3.989	284.6	−1.167	0.733	−0.321	0.221	−0.019	0.312	6.15	5.84
5	2.170	3.143	4.114	3.510	278.9	−1.130	0.721	−0.321	0.203	−0.016	0.319	13.57	13.06
6	2.166	3.144	4.323	2.545	279.1	−1.142	0.752	−0.319	0.194	−0.013	0.312	24.99	24.96
7	2.163	3.347	3.105	4.405	304.1	−1.237	0.899	−0.309	0.218	−0.002	0.017	13.98	14.25
8	2.151	3.336	4.994	4.356	305.2	−1.231	0.906	−0.338	0.162	0.000	0.008	17.69	18.14

[a] Values are averaged for each M or C′ unless otherwise noted. Relative stabilities (ΔE and ΔE^{high}) are referenced to the energies of **3**.

6-31G(d) for C and N and the relativistic effective core potential basis SDD[13] for La, as implemented in the *Gaussian 03* program.[14] We have used this approach in prior investigations of various late transition metal complexes.[15−17] To examine the performance of this method, geometry optimization was carried out for $Sc_3N@I_h$-C_{80}. The predicted key geometric parameters are in excellent agreement with experimental values.[18] For instance, the calculated average N−Sc bond length is 2.025 Å, to be compared with the experimental value 2.026 Å, and for the average Sc−Sc distance, we obtained 3.507 Å (expt: 3.499 Å). These results represent an improvement over prior reports.[19,20]

We first investigated the $C_{79}N$ cage alone to determine which site is preferred for N-substitution. In the I_h-C_{80}, there are two types of carbon atoms: 60 of them locate at junctions of two hexagons and one pentagon or 665 junction, while the remaining 20 atoms are located at junctions of three hexagons or 666 junction. Previous computational studies indicate N-substitutions at 665 junctions for $Y_2@C_{79}N$ and $Sc_3N@C_{79}N$ are the preferred sites.[21,22] However, it has not been revealed that such a preference is due to the metallofullerene formation or the intrinsic property of the $C_{79}N$ cage. Our calculations show that the 665 substitution isomer **1** of $C_{79}N$ is more stable by 13.19 kcal/mol than the 666 substitution isomer **2**. Interestingly, this value is close to the 13.3 kcal/mol energy difference reported previously for the two corresponding isomers of $Y_2@C_{79}N$,[22] indicating that such a preference observed in the metallofullerenes is essentially originated from the different stabilities of the two cage isomers alone. Indeed, as shown below for various $La_3N@C_{79}N$ isomers, very similar results were found. This trend of N-substitution for $C_{79}N$ is similar to that reported for $C_{69}N$,[23] which suggests that the 665 N-substitution preference might be inherent to fullerenes. It is also interesting to note that the N-substitution not only introduces a large negative charge on the cage (ca. −0.3 *e* at this N′ site) but also induces large positive charges (ca. 0.2 *e*) at its surrounding three carbon atoms (C′). All other carbon atoms in the $C_{79}N$ cage have small charges with absolute values <0.05 *e*. This unique property has an important effect on the relative stabilities of different isomers of $La_3N@C_{79}N$ (*vide infra*). Spin densities of the two isomers are all delocalized and mostly located at the opposite site of N-substitution; see Figure 3A and 3B.

We next investigated a number of extreme cases of possible isomers for the largest reported metallic nitride azafullerene $La_3N@C_{79}N$. With regard to the equatorial plane of the three metal atoms, we considered the N-substitution sites at both polar and equatorial regions. For polar substitutions, two isomers were investigated with the N′ atom (on the cage) and the N atom (on the La_3N cluster) separated in either closest (**3**) or farthest distances (**4**); see Figure 3C and 3D, respectively. For equatorial substitutions, isomers **5** and **6** were investigated; see Figure 3E and 3F. In **5**, the N′ atom is located between the two La atoms and in **6**, it faces one La atom directly. As seen from Table 1, among the four 665 substitution isomers, polar substitutions **3** and **4** are preferred over the equatorial ones **5** and **6**. The most stable isomer is **3**. This may seem counterintuitive since, in this conformation, the most negatively charged N atoms are in close proximity, which should impose large repulsion. However, as shown in Table 1, there are three La metals and three C′ atoms that have large positive charges, which also need to be separated as far as possible to avoid large repulsions. Among some key geometric parameters listed in Table 1, the minimum N′−M distance ($R_{N'M}^{min}$) can be used to evaluate such repulsions, as N′ is located in the center of the three C′ atoms. Long $R_{N'M}^{min}$ values indicate distant contacts between these six large

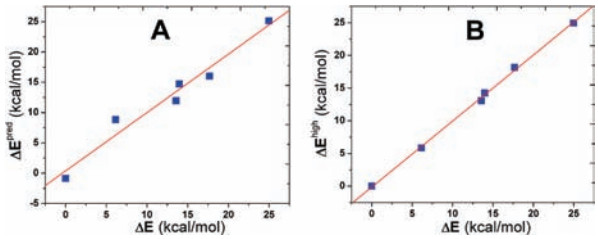

Figure 4. (A) Predicted stabilities from eq 1 vs DFT results. (B) Computed relative stabilities using high level methods vs those from low-level calculations.

positive charges, which are favored. Indeed, the linear correlation between stabilities of isomers **3**−**6** (ΔE) and $-R_{N'M}^{min}$ has an $R^2 = 0.977$ and $p = 0.01153$. The equatorial substituted isomer **6**, which has a direct contact between N′ and La atoms, results in large electrostatic repulsions and is the most unstable structure shown.

In addition, two polar N-substitutions at the 666 junction sites (**7** and **8**, see Figure 3G−H) were also investigated to compare with corresponding 665 isomers **3** and **4**. As shown in Table 1, the stability trend of 665 substitutions remains for 666 substitution isomers; i.e. the polar substitution with the closest N−N′ contact (or smallest $R_{NN'}$) is more stable than the farthest one. These results suggest that the relative stabilities of metallofullerene isomers is independent of the substitution junction sites: 665 or 666. The 666 substitution isomers are always less stable than the corresponding 665 ones. In fact, as shown in Figure 4A, the following regression yields excellent predictions of the stabilities of all isomers of $La_3N@C_{79}N$ with $R^2 = 0.967$ and $p = 0.00588$:

$$\Delta E = -14.409R_{N'M}^{min} + 1.245\,\delta_{5\text{-}6} + 62.53 \qquad (1)$$

where δ_{5-6} is 0.00 kcal/mol for 665 substitution isomers and 13.19 kcal/mol (the energy difference between the 665 and 666 isomers of $C_{79}N$ cage) for 666 isomers. This shows the difference between corresponding conformations in 665 and 666 isomers originates essentially from the cages.

To examine if this trend could be affected by different levels of theory, additional high level single-point energy calculations were also performed with more polarization and diffuse functions for C and N, i.e. the 6-31+G(2d) basis, which results in 2205 basis functions. As seen from Table 1, the relative stabilities at this level (ΔE^{high}) are basically the same as ΔE. In fact, the correlation shown in Figure 4B has an $R^2 = 0.998$, slope = 1.01, intercept = −0.15 kcal/mol, and $p < 0.0001$. These electronic results further validate our method, in addition to the excellent predictions of geometric results discussed above for $Sc_3N@C_{80}$.

Compared to 665 isomers of $La_3N@C_{79}N$, in those 666 isomers, the La_3N cluster is more compressed, as shown by the relatively shorter N−M distance (R_{NM}), longer M−M distance (R_{MM}), and larger sum of three M−N−M angles ($\Sigma\angle$MNM) in Table 1. Interestingly, spin density distributions among these two types of N-substituted isomers are distinctive. As seen from Table 1 for Mulliken spin densities of N and M atoms (ρ_N and ρ_M) in the La_3N fragment of the metallofullerene and Figure 3C−F, in all 665 isomers (**3**−**6**), the unpaired electrons reside in the La_3N cluster, while, in all 666 isomers (**7**−**8**), the unpaired electrons are delocalized in the cage. It is also interesting to note that in $La_3N@C_{79}N$, the spin-containing orbital is the HOMO in all isomers, as shown in Figure 5A−F for isomers **3**−**8**. This is in contrast with a previous investigation of $Y_2@C_{79}N$, in which the spin-containing orbital is below the HOMO.

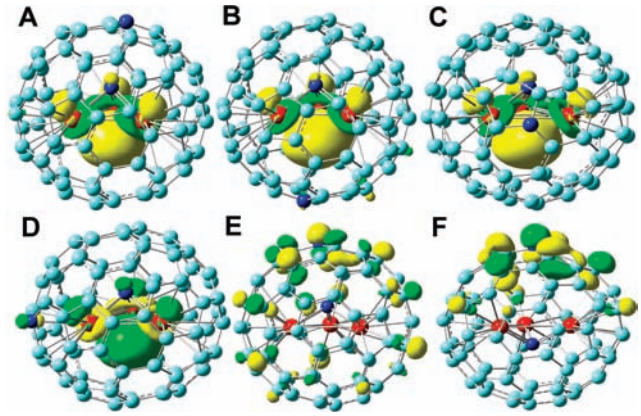

Figure 5. Isosurface representations (**A**−**F**) of HOMOs in $La_3N@C_{79}N$ isomers **3**−**8**, respectively (contour values = ± 0.04 au).

Acknowledgment. Y.Z. thanks NSF EPSCoR Award OIA-0556308, the Mississippi Center for Supercomputing Research, the USM Vislab for computing facilities, and Brian Hopkins for technical assistance. S.S. thanks NSF CHE-0547988. J.P.P. thanks NSF CHE-0847481. H.D. thanks NSF DMR-0507083 and NIH 1R01-CA119371-01.

Supporting Information Available: Full citation of ref 14 and optimized geometries of **1**−**8** (Tables S1−S8). This material is available free of charge via the Internet at http://pubs.acs.org.

References

(1) Stevenson, S.; Rice, G.; Glass, T.; Harich, K.; Cromer, F.; Jordan, M. R.; Craft, J.; Hadju, E.; Bible, R.; Olmstead, M. M.; Maitra, K.; Fisher, A. J.; Balch, A. L.; Dorn, H. C. *Nature* **1999**, *401*, 55–57.
(2) Chaur, M. N.; Athans, A. J.; Echegoyen, L. *Tetrahedron* **2008**, *64*, 11387–11393.
(3) Dunsch, L.; Yang, S. *Small* **2007**, *3*, 1298–1320.
(4) Dunsch, L.; Yang, S. F. *Phys. Chem. Chem. Phys.* **2007**, *9*, 3067–3081.
(5) Stevenson, S.; Fowler, P. W.; Heine, T.; Duchamp, J. C.; Rice, G.; Glass, T.; Harich, K.; Hajdu, E.; Bible, R.; Dorn, H. C. *Nature* **2000**, *408*, 427–428.
(6) Olmstead, M. H.; de Bettencourt-Dias, A.; Duchamp, J. C.; Stevenson, S.; Marciu, D.; Dorn, H. C.; Balch, A. L. *Angew. Chem., Int. Ed.* **2001**, *40*, 1223–1225.
(7) Melin, F.; Chaur, M. N.; Engmann, S.; Elliott, B.; Kumbhar, A.; Athans, A. J.; Echegoyen, L. *Angew. Chem., Int. Ed.* **2007**, *46*, 9032–9035.
(8) Chaur, M. N.; Melin, F.; Elliott, B.; Kumbhar, A.; Athans, A. J.; Echegoyen, L. *Chem.—Eur. J.* **2008**, *14*, 4594–4599.
(9) Chaur, M. N.; Valencia, R.; Rodriguez-Fortea, A.; Poblet, J. M.; Echegoyen, L. *Angew. Chem., Int. Ed.* **2009**, *48*, 1425–1428.
(10) Chaur, M. N.; Melin, F.; Ashby, J.; Elliott, B.; Kumbhar, A.; Rao, A. M.; Echegoyen, L. *Chem.—Eur. J.* **2008**, *14*, 8213–8219.
(11) Stevenson, S.; Thompson, M. C.; Coumbe, H. L.; Mackey, M. A.; Coumbe, C. E.; Phillips, J. P. *J. Am. Chem. Soc.* **2007**, *129*, 16257–16262.
(12) Adamo, C.; Barone, V. *J. Chem. Phys.* **1998**, *108*, 664–675.
(13) Leininger, T.; Nicklass, A.; Stoll, H.; Dolg, M.; Schwerdtfeger, P. *J. Chem. Phys.* **1996**, *105*, 1052–1059.
(14) Frisch, M. J.;et al. *Gaussian 03*, revision D.01; Gaussian, Inc.: 2004.
(15) Balof, S. L.; Yu, B.; Lowe, A. B.; Ling, Y.; Zhang, Y.; Schanz, H. J. *Eur. J. Inorg. Chem.* **2009**, 1717–1722.
(16) Zhang, Y.; Guo, Z. J.; You, X. Z. *J. Am. Chem. Soc.* **2001**, *123*, 9378–9387.
(17) Zhang, Y.; Lewis, J. C.; Bergman, R. G.; Ellman, J. A.; Oldfield, E. *Organometallics* **2006**, *25*, 3515–3519.
(18) Stevenson, S.; Lee, H. M.; Olmstead, M. M.; Kozikowski, C.; Stevenson, P.; Balch, A. L. *Chem.—Eur. J.* **2002**, *8*, 4528–4535.
(19) Kobayashi, K.; Sano, Y.; Nagase, S. *J. Comput. Chem.* **2001**, *22*, 1353–1358.
(20) Wu, J.; Hagelberg, F. *J. Phys. Chem. C* **2008**, *112*, 5770–5777.
(21) Hou, J. Q.; Kang, H. S. *Chem. Phys.* **2007**, *334*, 29–35.
(22) Zuo, T. M.; Xu, L. S.; Beavers, C. M.; Olmstead, M. M.; Fu, W. J.; Crawford, D.; Balch, A. L.; Dorn, H. C. *J. Am. Chem. Soc.* **2008**, *130*, 12992–12997.
(23) Hou, J. Q.; Kang, H. S. *J. Phys. Chem. A* **2007**, *111*, 1111–1116.

JA908370T